Mathematical Biology and Bioinformatics
2023. V. 18. № S. P. t94–t106. doi: 10.17537/2023.18.t94

Ttranslation of the original article
Medvedev A.E., Erokhin A.D. Mathematical Biology and Bioinformatics. 2023;18(2):464–478. doi: 10.17537/2023.18.464

========== TRANSLATIONS OF PUBLISHED ARTICLES ==========

Mathematical analysis of aortic deformation in aneurysm and wall dissection

Medvedev A.E.[1, 2], Erokhin A.D.[1]

[1]*Khristianovich Institute of Theoretical and Applied Mechanics Siberian Branch of the Russian Academy of Sciences, Novosibirsk, Russia*
[2]*E. Meshalkin National Medical Research Center of the Ministry of Health of the Russian Federation, Novosibirsk, Russia*

Abstract. Aortic dissection is an extremely severe pathology. From the viewpoint of mechanics, the aorta is a multilayered anisotropic reinforced shell, which is subjected to periodic loading under the action of pulsed blood pressure. Various issues of mathematical modeling of dissection of the aorta and large arteries are considered in the present study. Modern mathematical models of the aortic and arterial wall structures obtained by processing experimental data on biaxial stretching of samples are reviewed. These mathematical models can be conventionally divided into two classes: 1) effective models, where the internal structure of the walls is ignored, but mechanical parameters of the material "averaged" over the wall thickness are introduced; 2) structured models, which take into account the multilayered (up to three layers) structure of the artery with addition of one to four families of reinforcing fibers. One of the most popular models (Holzapfel-Gasser-Ogden model) is considered in detail. This model describes a two- or three-layered artery with two families of reinforcing fibers. For this model, tables of design parameters are provided, and numerical simulations of arterial rupture and dissection are performed. The blood vessel is subjected to pulse pressure of blood flowing through it. It is shown that rupture of the inner layer of the vessel leads to an increase in the stress at the outer wall of the vessel. As the rupture thickness and length increase, the stress at the outer wall of the vessel is also increased. If there is an aneurism of the vessel, the stress is twice that in the vessel without the aneurism. Dissection of the inner wall of the vessel leads to an increase in the stress at the wall: the stress decreases with increasing rupture width for a straight vessel and increases for a vessel with an aneurism. The stress calculations on the "tip" of delamination show that the maximum stress is reached at the outer wall of the rupture.

Key words: *aorta dissection, aortic aneurism, mathematical modeling, hemodynamics, wall stress, biomechanics.*

INTRODUCTION

Aorta dissection is an extremely severe pathology [1]. This is a sufficiently rare, but potentially dangerous disease, which is encountered in 1 out of 10000 hospitalized patients. Many patients die before hospitalization: 3–4 % of all sudden deaths due to cardiovascular diseases [2]. Without medical treatment, premature mortality for patients with dissection is 1 % per hour (one patient out of 100 dies each hour) at the first day, 75 % during two weeks, and 90 % during the first year. However, survivability of patients can be appreciably increased owing to early diagnosis and medical treatment of this severe disease.

From the mechanical viewpoint, the aorta is a multilayered thick-walled shell (Fig. 1). There three basic layers: intima, media, and adventitia. The intima produces a minor effect on the mechanical properties of the aorta wall [1]. Therefore, mathematical models often deal with a two-layer aorta consisting of the inner (media) and outer (adventitia) layers.

We are interested in physical aspects of the behavior of the aorta walls with an aneurism and/or dissection under the action of a pulse blood flow in the vessel. Such studies were performed earlier. Zorrilla et al. [3] applied a CFD method to study a fluid flow in a model configuration simulating aorta dissection. It was shown that the flow structure agrees well with available *in vitro* experiments.

For mathematical modeling of aorta dissection, one has to design a geometrical model of the aorta. Medvedev [4] in earlier studies developed a method for aorta model construction (including the aortic root, thoracic aorta, aortic arch with branches, and abdominal aorta with vessel bifurcations) by analytical formulas. The parameters of these formulas allow one to "fit" the constructed aorta shape to specific features of the aorta of an individual patient. The resultant three-dimensional (3D) aorta model is completely ready for 3D simulations and for printing on a 3D printer. Another approach to aorta model construction was proposed by Mistelbauer et al. [5]. They used a method of retrieval of the aorta cross section with dissection from computer tomography results. The data retrieval was performed on the basis of elliptical Fourier descriptors. In contrast to the traditional method based on splines, the use of the Fourier descriptors makes it possible to control the accuracy of aorta dissection and is a step forward to automated generation of surface models of aorta dissection.

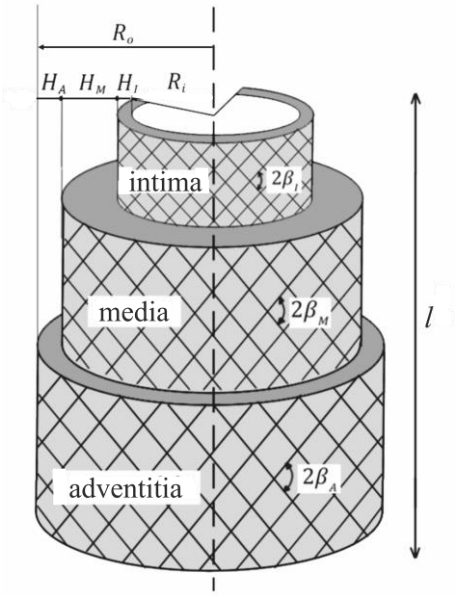

Fig. 1. Structure of aorta walls in accordance with the 3D model [20]. Here l is the length of the aorta segment, R_i and R_o are the inner and outer radii of the aorta, H_A is the adventitia layer thickness, H_M is the media layer thickness, H_I is the intima layer thickness, and β_A, β_M, and β_I are the angles of inclination of the reinforcing fibers of the adventitia, media, and intima, respectively.

Aorta pathology alters the strength properties of the vessel walls. Jadaun and Nitin [6] used the mathematical apparatus of the Lie transformation group to analyze the nonlinear wave dynamics of wave propagation in the aorta walls. It was found that aorta dissection serves as a trigger of disease progressing at the early stage due to the formation of soliton-like pulses and their interaction. Emerel et al. [7] performed computer angiography with simultaneous estimation of the arterial pressure for two groups of patients. As a result, it became possible to measure: 1) aorta motion during the cardiac cycle; 2) peripheral arterial pressure (moreover, the pressure was measured by a noninvasive method). For the first group,

aorta dissection was diagnosed later on; the second (control) group was composed of patients with a presumably normal aorta with no dissection. Based on these data superimposed onto the aorta geometry obtained by computer angiography, local stresses in the aorta wall were calculated, both axial (longitudinal) stresses and circumferential (radial) stresses, which are usually significantly lower than axial stresses. The results were compared to data obtained in the control group. It was found that 1) elasticity of the ascending thoracic aorta was lower, while the stiffness was higher in those aortas that finally experienced dissection; 2) calculated axial normal stresses (not circumferential stresses) were higher in aortas that experienced dissection; 3) input ruptures appeared in zones with high calculated axial normal stresses. The main conclusion made in [7] can be formulated as follows: local axial (longitudinal) normal stresses can be more important for thoracic aorta pathogenesis that circumferential (radial) normal stresses. This conclusion differs from that drawn in available publications.

Lipovka et al. [8] studied the strength characteristics of the human aorta tissues and aneurism, as well as iliac arteries. It was experimentally proved that the difference in the limiting relative strains in the axial and tangential directions in healthy aorta tissue samples is statistically significant, which is not the case for the aorta aneurism. The results can be also treated as the fact of remodeling of the aorta aneurism wall as compared to a healthy aorta. These data can be used in problems of personalized hydroelastic modeling for constructing predictive models of rupture of aneurisms of this kind.

MECHANICAL PROPERTIES OF THE AORTA

Arteries (in particular, aorta) are blood vessels that transport fresh blood saturated with oxygen from the heart over the entire body. The arterial wall consists of four basic components: muscles, elastin, collagen, and fibroblasts. Muscles are active components of the artery wall, which also affect the geometry and elastic properties of the artery. Elastin is a rubber-type material made of protein in a polymerized form, which is elastic and can endure high stresses and strains. Collagen fibers ensure necessary strength of the arterial wall and are responsible for the nonlinear elastic behavior of the wall at high strains. At lower strains, the fibers roll up and do not make any significant contribution to elastic properties of the vessel. Fibroblasts exhibit a gel-like viscous behavior, and their contribution to wall elasticity is usually ignored. A histological analysis of an artery segment makes it possible to identify three individual layers called tunics: intima, media, and adventitia, as shown in Fig. 1. If there is a vascular disease, e.g., atherosclerosis, the mechanical properties of the damaged layers of the arterial wall are appreciably different from the mechanical properties of the healthy artery [6–8].

The aorta walls are characterized by the following mechanical properties.

Incompressibility. The experimental measurements show that the arterial wall is almost incompressible. The results of [9, 10] showed that the change in the volume was only 0.165 % for the arterial segment stretched *in vivo* by a pressure of 181 mmHg.

Anisotropy. The mechanical behavior of the arterial wall is anisotropic [11, 12].

High nonlinear deformations. The aorta walls experience high deformations under the action of the blood pressure. The deformation induced by pressure changes during the cardiac cycle can reach 10–15 % of the initial volume of the aorta [11, 12]. The wall is easily deformed at low pressures, while it becomes stiff at higher pressures.

Viscoelasticity. The stressed state of the wall is determined not only by the corresponding deformation, but also by previous deformations. The wall components cannot be considered as elastic anymore; therefore, they have to be considered as a viscoelastic material [13].

To describe the behavior of arteries under loading, it is necessary to develop mathematical models of the blood vessel. Sevel models that deserve attention are described in available publications.

Model without reinforcement of the artery walls [14]. A three-dimensional stress-strain dependence derived on the basis of the strain energy function was proposed for the arterial wall. The model constants were determined from experimental data on rabbit arteries subjected to blowing and longitudinal stretching in the physiological range.

Single-fiber model [15, 16]. It was shown that the existing slope of the smooth muscle fibers is optimal from the viewpoint of the vessel strength.

Four-fiber model [17, 18]. A single-layer model with four families of collagen fibers was proposed. It was noted that a family of four fivers reflects the two-ax mechanical behavior of the human abdominal aorta with or without aneurism for patients from 30 to 60 years old.

Three-layer orthotropic model [19]. Bending stability of a rectilinear segment of the aorta with a blood flow was studied. It was noted that the systole-diastole cycle or intense physical exercise, which lead to permanent oscillations of the aorta, combined with cardiovascular diseases or other pathological problems, can provoke the aneurism emergence and growth or aorta dissection.

Two-fiber two- or three-layer Holzapfel-Gasser-Ogden (HGO) model [20–23]. The reinforced three-layer aorta described by the HGO model is schematically shown in Figure 1. The constitutive HGO model reflects the anisotropic nonlinear mechanical response observed in experiments on cutout arteries. This model is widely used to describe the behavior of biological tissues [24, 25].

Three-layer model [25]. The model takes into account three layers of the artery: intima, media, and adventitia. Based on the HGO model, a new computational approach was proposed, where the mechanical properties of each of the three layers of the aorta determined experimentally in simple and available one-axis tests, are use to formulate a three-layer model of the arterial wall.

Effective model of the blood vessel [26]. Based on a procedure of dimension reduction for a three-dimensional system of elasticity equations, a two-dimensional model of an elastic layered wall of the blood vessel was developed. Explicit formulas for the effective tensor of wall stiffness in two natural cases were derived.

MATHEMATICAL MODELING OF AORTA WALLS

The anisotropic properties of the aorta structure were modeled with the use of the two-layer HGO model of an incompressible anisotropic material [20]. This model implies that the media and adventitia are hyperelastic materials reinforced with two families of fibers.

A hyperelastic material is determined by the elastic strain energy density W_S, which is a function of the elastic strain state. It is often called the *energy density*. The hyperelastic formulation usually yields a nonlinear stress-strain dependence, in contrast to Hooke's law in linear elasticity.

In most cases, the current strain state is described with the use of the *right Cauchy-Green strain tensor* C (though it is also possible to use the *left Cauchy-Green tensor* B, strain gradient tensor F, etc.); therefore, the strain energy density is written as $W_S(C)$.

For isotropic hyperelastic materials, any strain state can be described in terms of three independent variables: the most frequently chosen variables are the *invariants* of the right Cauchy-Green tensor C, the invariants of the Green-Lagrange strain tensor, or the *principal directions*. After determining the strain energy density, the Piola-Kirchhoff stress tensor of the second kind is calculated as

$$S = 2\frac{\partial W_S}{\partial C}. \tag{1}$$

The following assumptions are used in the HGO model [20] to describe the deformation of the blood vessels. Hyperelasticity is considered within the framework of the neo-Hookean

model (nonlinear elasticity). The isochoric (constant-volume) strain energy density is determined by the function

$$W_{HGO} = W_{nH} + W_{fib,1} + W_{fib,2}\,. \tag{2}$$

The elastic strain energy density of the neo-Hookean material is

$$W_{nH} = \frac{\mu}{2}\left(I_1 - 3\right), \tag{3}$$

where μ is the shear modulus, and I_1 is the first invariant of the strain tensor C.

The second and third terms in the right-hand side of Eq. (2) describe the mechanical contribution of the collagen fiber network. In accordance to the model [20], these expressions are written as

$$W_{fib,m} = \frac{k_1}{2k_2}\left[e^{Q_{fib,m}} - 1\right],\ Q_{fib,m} = k_2\left[k_3\left(I^{(1)}_{fib,m} - 3\right) + \left(1 - 3k_3\right)\left(I^{(4)}_{fib,m} - 1\right)\right]^2. \tag{4}$$

Here the fiber network is reduced to two $\left(m = 1,2\right)$ families of fibers with the material properties k_1, k_2, and k_3. The deformation of each family of fibers is measured by the first $I^{(1)}_{fib,m}$ and fourth $I^{(4)}_{fib,m}$ invariants of the right strain tensor $C_{fib,m}$ of the collagen fiber family with the orientation $\left\{-\beta,\beta\right\}$. The invariants of the strain tensor of the fibers are

$$I^{(1)}_{fib,m} = \mathrm{trace}\left(C_{fib,m}\right),\ I^{(4)}_{fib,m} = \lambda^2_{fib,m},\ m = 1,2\,, \tag{5}$$

The first invariants of Eq. (5) are the traces of the matrix $C_{fib,m}$. The fourth invariant of Eq. (5) is a quadratic value of the isochoric elastic tension in the fiber direction $\left\{-\beta,\beta\right\}$. For biological tissues, it is assumed that the fibers can endure compression; therefore, the fiber stiffness is added only in the case of stretching, i.e., $\lambda_{fib,1} > 1$ and $\lambda_{fib,2} > 1$.

Based on the strain energy density (2), it is possible to calculate the Piola-Kirchhoff stress tensor of the second kind by the formula

$$S_{HGO} = S_{nH} + S_{fib,1} + S_{fib,2}\,, \tag{6}$$

where the Piola-Kirchhoff tensor of the second kind for the binder is calculated by formula (1) as

$$S_{mP} = \frac{\partial W_{mP}}{\partial C}\,, \tag{7}$$

and the stress contribution from each family of fibers is determined as

$$S_{fib,m} = 2\frac{\partial W_{fib,m}}{\partial C},\ m = 1,2\,. \tag{8}$$

Tables 1–4 show the parameters for calculating arteries (aortas) by the two-layer (Tables 1 and 3) and three-layer (Tables 2 and 4) HGO models. The contributions of the collagen fiber network to energy in Tables 1, 2, and 3 are calculated by formula (4). The calculations based on the data from Table 4 are performed by a modified formula of the contribution of the collagen fibers [22]:

$$W_{fib,m} = \frac{k_1}{2k_2}\left[e^{Q_{fib,m}} - 1\right],\ Q_{fib,m} = k_2\left[\left(1 - k_3\right)\left(I^{(1)}_{fib,m} - 3\right)^2 + k_3\left(I^{(4)}_{fib,m} - 1\right)^2\right]. \tag{9}$$

Table 1. Parameters of the HGO model [20] for rabbit's carotid artery with the inner radius $R_i = 0.71$ mm and outer radius $R_o = 1.1$ mm

Material properties	Media	Adventitia
μ , kPa	3	0.3
k_1 , kPa	2.3632	0.5620
k_2	0.8393	0.7112
k_3	0	0
β , deg	29	62
H , mm	0.26	0.13

Table 2. Parameters of the HGO model [25] for pig's upper thoracic aorta. The layers occupy 14, 59, and 27% of the aorta wall thickness, respectively. The inner radius is $R_i = 8.66$ mm, and the outer radius is $R_o = 10.95$ mm

Material properties	Intima	Media	Adventitia
μ , kPa	47	44.6	42.4
k_1 , kPa	249.4	269.6	51.4
k_2	11	9.5	67.3
k_3	0.24	0.24	0.18
β , deg	39.5	33.4	42.9
H , mm	0.33	1.35	0.61

Table 3. Parameters of the HGO model [21] for the left human frontal coronary artery with the inner radius $R_i = 3.302$ mm and outer radius $R_o = 3.729$ mm

Material properties	Media	Adventitia
μ , kPa	27.0	2.7
k_1 , kPa	0.64	5.1
k_2	3.54	15.4
k_3	0	0
β , deg	10	40
H , mm	0.493	0.247

Table 4. Parameters of the HGO model [22] for the left human frontal coronary artery with the inner radius $R_i = 3.47$ mm and outer radius $R_o = 4.5$ mm

Material properties	Intima	Media	Adventitia
μ , kPa	55.8	2.54	13.12
k_1 , kPa	527.32	43.2	77.14
k_2	170.88	8.21	85.03
k_3	0.51	0.25	0.55
β , deg	60.3	20.61	67.0
H , mm	0.27	0.36	0.40

The mechanical properties of arteries depend on many factors (age, pathologies, etc.) [7]; this fact is responsible for the large differences in the arterial parameters listed in Tables 1–4.

In addition to the functions $W_{fib,m}$ of the elastic strain energy of collagen fibers (formulas (4) and (9)) considered here, there are also some other functions [17, 18, 27, 28]. Ngwangwa et al. [29] experimentally verified six different forms of the functions $W_{fib,m}$ of the elastic strain energy of collagen fibers, though these functions were verified for soft tissues of sheep esophagus. Significant differences were observed between experimental and numerical data for different models of the elastic strain energy. Ngwangwa et al. [29] concluded that the best description of experimental data (for soft tissues of sheep esophagus) is provided by the four-fiber model [18].

RESPONSE OF THE AORTA WALLS WITH RUPTURE AND ANEURISM TO PULSE PRESSURE OF THE BLOOD FLOW

The pulse pressure of the blood flow generates a load onto the aorta. If there are some defects of the aorta (dissection or aneurism), this load leads to high stresses at the aorta wall at those places where these defects are located. Roy et al. [30] presented a review of mathematical methods used to study the loads onto the aorta walls in the case with an aneurism. It was noted that one of the basic currently used methods is computer simulation. The limiting loads onto the aorta were studied in [31], where it was experimentally found that the limiting and yield (irreversible inelastic damage) stresses in the axial direction for a healthy aorta are 0.75 and 1 MPa, respectively; the corresponding stresses in the circumferential direction are 1 and 1.2 MPa, respectively. The yield stress is understood here as the stress of the beginning of irreversible fracture of the aorta.

The blood flow in a pathological aorta with the wall deformation being ignored was investigated by many researchers: a review of such studies can be found in [32]. Shi et al. [33] performed a numerical study of the load on the aorta wall with dissection, where the wall deformation was ignored (the aorta walls were assumed to be rigid and nondeformable).

A segment of the rabbit's carotid artery was calculated (Table 1). The following technique was used to calculate the deformation and the load on the aorta in the case with pulsed motion of blood (Fig. 2).

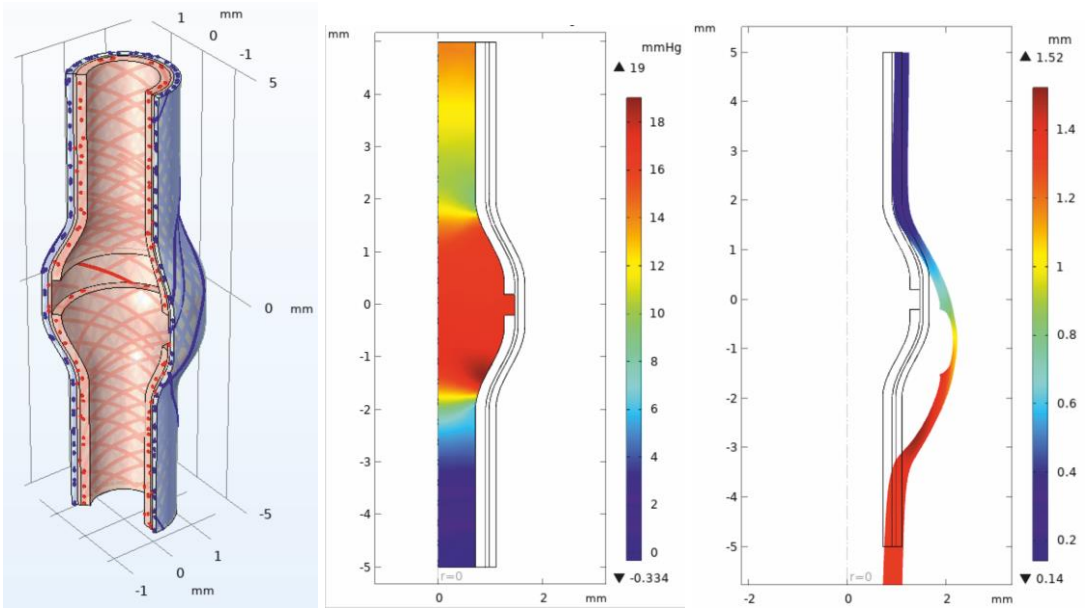

Fig. 2. Three stages of the method of calculating the load on the artery: **a**) construction of the reinforced structure of the arterial walls; **b**) calculation of the blood flow in one pressure pulse; **c**) calculation of the strain and stress in the arterial walls under the action of the load generated by the pulse blood flow in the vessel.

At the first stage, a multilayered (two- or three-layer) reinforced structure of the aorta walls was constructed (Fig. 2,a).

The second stage was calculation of an unsteady blood flow in a nondeformed aorta (Fig. 2,b). The blood motion was described by the model of a viscous incompressible fluid with a density of 1060 kg/m^3 and dynamic viscosity coefficient of 0.005 Pa·s. The use of the model of a non-Newtonian fluid does not make much sense: we consider a sufficiently short local segment of the artery, where the non-Newtonian properties of blood do not have enough time to manifest themselves and affect the pressure at the vessel wall. The flow rate of blood in the artery is defined by the formula $Q(t)=Q_{max}\dfrac{1-\cos(5\pi t)}{2}$, where the maximum flow rate is $Q_{max}=4$ ml/s, and the time of one pulse is 0.4 s. We are interested in the maximum load on the artery wall (the maximum load is reached at $t=0.2$ s); therefore, the pulse shape is not very important. This is the reason for the pulse function choice. The calculation time, flow rate, and pressure correspond to one cycle of the blood pulse: the maximum difference in the pressure at the vessel input and output is 40 mmHg.

The third stage (Fig. 2,c) is the calculation of the strains and stresses at the vessel walls under the action of the load determined at the second stage. The calculations were performed on the basis of the two-layer HGO model (the calculation parameters are listed in Table 1. The maximum (in terms of time and vessel length) Mises stresses at the outer wall of the artery in the case of rupture of the inner layer of the media were calculated (Fig. 3). The maximum stress was reached at the time instant of 0.2 s (at the middle of the cardiac cycle of the blood pulse) and at a point near the middle of the rupture (point with the coordinate $z=0$ in Fig. 2,a). An artery segment 10 mm long was considered. The aneurism height (Fig. 3,b) was $R_o/2$. The media rupture length L was varied from 0 to 0.8 mm, and the rupture thickness h was calculated for the values of 1/3, 1/2, 2/3, 5/6, and 1 of the media thickness H_M. The calculations were performed for a straight artery (Fig. 3,a) and an artery with an aneurism (Fig. 3,b). The results are presented for an artery with rupture (Fig. 3) and for an artery with rupture and media dissection (Fig. 4). The inner radius of media dissection is $L_d=0.75R_i$. The maximum stresses for a straight artery (Figs. 3,a and 4,a) and an artery with an aneurism (Figs. 3,b and 4,b) are compared.

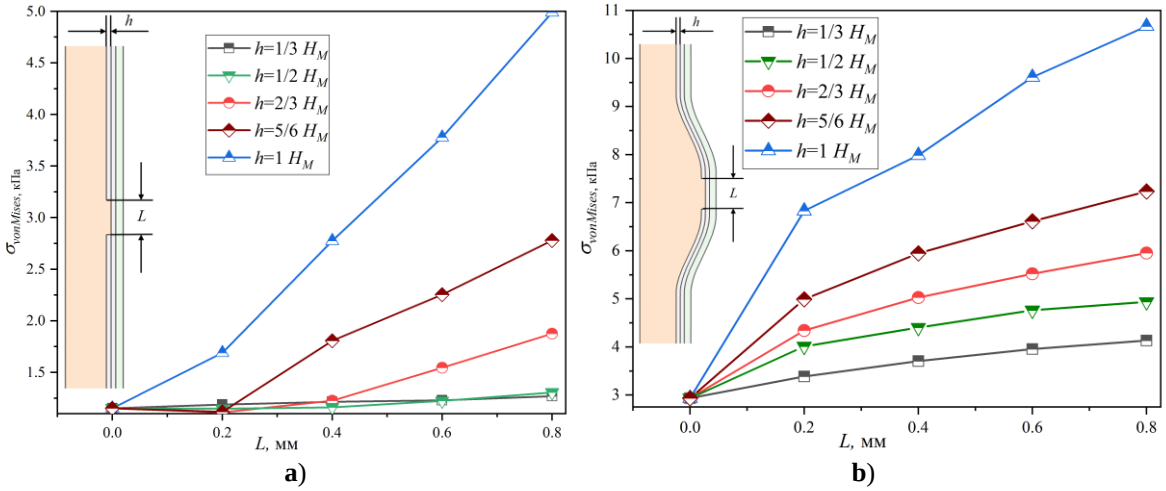

Fig. 3. Maximum Mises stresses $\sigma_{vonMises}$ at the outer wall of the artery versus the media dissection length L for a straight artery (**a**) and an artery with an aneurism (**b**). The rupture thickness h is 1/3, 1/2, 2/3, 5/6, and 1 of the media thickness H_M.

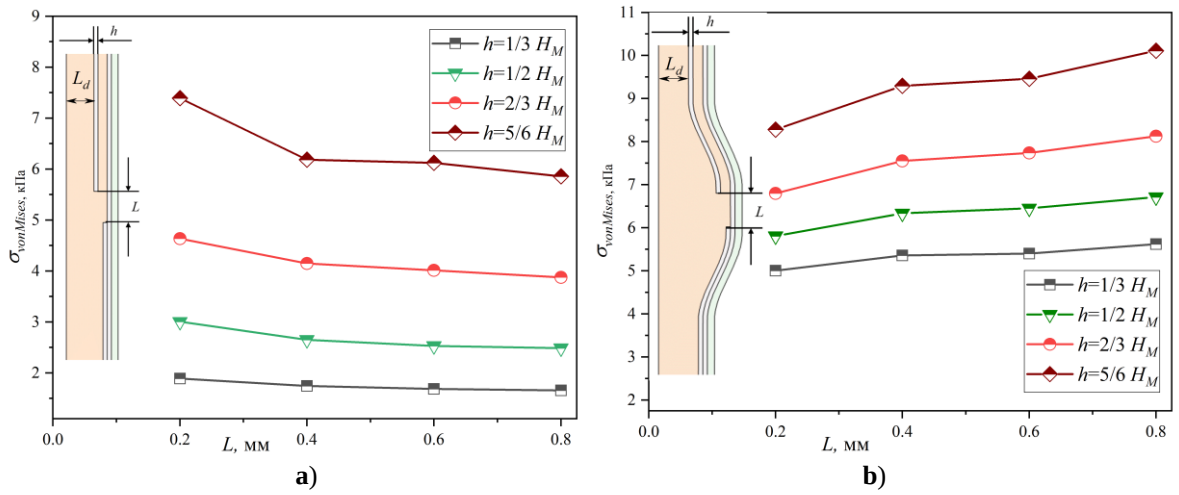

Fig. 4. Maximum Mises stress $\sigma_{vonMises}$ at the outer wall of the artery with dissection versus the media rupture length L for a straight artery (**a**) and an artery with an aneurism (**b**). The rupture region thickness h is 1/3, 1/2, 2/3, and 5/6 of the media thickness H_M.

It is seen from Fig. 3 that an increase in the aorta wall rupture length L leads to an increase in pressure at the outer wall. The presence of an aneurism increases the stress at the outer wall of the artery almost by a factor of 2 (Figs. 3,a and 3,b).

For the aorta with dissection (Fig. 4), the stress pattern is different. For a straight aorta, and increase in the aorta wall rupture length L leads to a decrease in the stress at the outer wall (Fig. 4,a), while the presence of an aneurism increases the stress at the outer wall of the artery with an increase in the rupture length L (Fig. 4,b). In this case, the stress in the aorta with an aneurism (Fig. 4,b) is only slightly higher than that in the straight aorta (Fig. 4,a). Aorta dissection is responsible for a significant (almost by a factor of 1.5) increase in the stress at the outer wall of the aorta (cf. Figs. 3 and 4).

Three-dimensional calculations of artery dissection due to calcification were performed (Fig. 5).

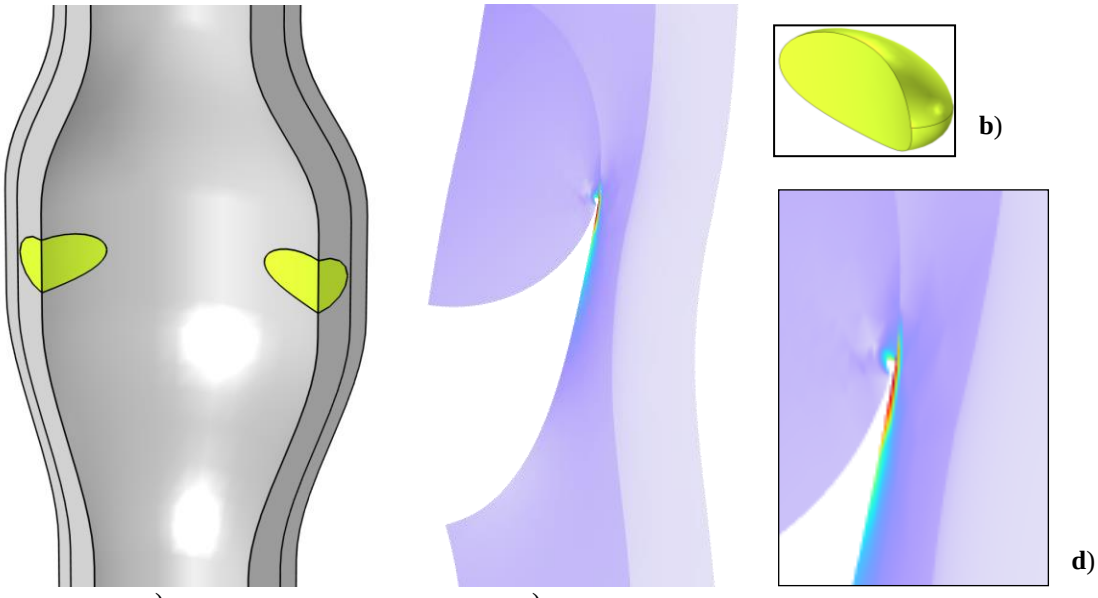

Fig. 5. Modeling of artery dissection due to calcification of a media wall fragment. **a**) One quarter of the longitudinal section of the vessel with calcification plaques (marked yellow. **b**) General view of the calcification plaque. **c**) Stresses and strains of the aorta wall with dissection over the calcification plaque boundary. **d**) Magnified pattern of the stress at the dissection crack tip (the red color indicates the maximum stress at the outer boundary of the rupture).

MODELING OF DISSECTION OF AORTA WALLS DUE TO CALCIFICATION

One of the reasons for aorta dissection is calcification of vessel walls. Li et al. [34] used a numerical method to study the relationship between the stress in the aorta wall and the calcification volume. It was shown that calcification increases the peak pressure of the aorta wall, which testifies to reduction of biomechanical stability of the arterial wall. Kumara and Faye [35] performed numerical simulation of the influence of calcification on the strength of the aorta aneurism wall. Circular and elliptical calcification particles with various volume fractions were used for modeling. The goal of [35] was to predict the calcified aneurism rupture under biaxial loading for various tension coefficients. The evolution of aorta dissection under the action of internal pressure was considered in [36]. An initial rupture affected by internal pressure was set inside the artery. Quasi-static solutions were calculated to determine the critical pressure at which dissection propagation begins. The model [36] shows that dissection displays a trend of radial outward propagation.

Aorta dissection in the case of partial calcification of the artery was calculated (Fig. 5). Four segments of the arterial wall with an aneurism were subjected to calcification. Figure 5,a shows one quarter of the artery, while the form of the calcification region is shown in Figure 5,b Elliptical calcification regions were considered in [35]. It was assumed in the calculation than artery dissection has already arrived at the boundary of the all calcification regions (Figs. 5,c and 5,d). The stress at the tip was also calculated. It is seen from Figures 5,c and 5,d that the stress reaches the maximum value (denoted by the red color) at the outer side of the rupture; this fact confirms the conclusions of [36] about the trend of radial outward propagation of dissection.

CONCLUSIONS

Several issues of mathematical modeling of dissection of the aorta and large arteries are considered. Available mathematical models of the structure of aorta and arterial walls are reviewed. The most complicated models describe a three-layer (intima, media, and adventitia) structure of the vessel walls. In some cases, the models deal only with a two-layer (media and adventitia) structure of the walls because intima does not produce any significant effect on the mechanical properties of the vessel. Nonlinearity and anisotropy of the elastic properties of the vessel wall layers require the models to become more comprehensive: the collagen fibers of the vessel walls are modeled by two (or even four) families of the neo-Hookean (nonlinearly elastic) fibers intersecting at certain angles. The complexity of the mathematical models requires many (up to 18, see Tables 1 and 4) mechanical characteristics of the vessel wall materials to be determined. A review of available publications on vessel wall parameters for two- and three-layer vessel models based on one of the most popular artery models, i.e., the Holzapfel-Gasser-Ogden (HGO) model [20–23] is made.

The artery rupture and dissection are numerically simulated on the basis of the HGO model. In this study, the blood vessel is subjected to pulse pressure of the blood flow inside. It is shown that the rupture of the inner layer of the vessel leads to an increase in the stress at the outer wall of the vessel. An increase in the rupture thickness and length leads to an increase in the stress at the outer wall of the vessel. Because of the presence of an aneurism, the stress is twice that in the vessel with no aneurism. Dissection of the inner wall of the vessel leads to an increase in the stress at the wall: the stress decreases with increasing rupture width for a straight vessel and increases for a vessel with an aneurism. The stress calculations at the dissection “tip” show that the maximum stress is reached at the outer wall of the vessel.

The study was supported by the Russian Science Foundation (Grant No. 22-15-20005).

REFERENCES

1. Melissano G. *Aortic dissection: Patients true stories and the innovations that saved their lives*. Milan, Italy: Edi. Ermes, 2016. 439 p.
2. Razumova E.T., Lusov V.A., Kokorin V.A. Aortic dislayering. *Russian Journal of Cardiology*. 2001. V. 31. No. 5. P. 88–94 (in Russ.).
3. Zorrilla R., Soudah E., Rossi R. Computational modeling of the fluid flow in type B aortic dissection using a modified finite element embedded formulation. *Biomechanics and Modeling in Mechanobiology*. 2020. V. 19. P. 1565–1583. doi: 10.1007/s10237-020-01291-x
4. Medvedev A.E. Construction of complex three-dimensional structures of the aorta of a particular patient using finite analytical formulas. *Mathematical Biology and Bioinformatics*. 2022. V. 17. No. S. P. t30–t41. doi: 10.17537/2022.17.t30
5. Mistelbauer G., Rössl C., Bäumler K., Preim B., Fleischmann D. Implicit modeling of patient-specific aortic dissections with elliptic Fourier descriptors. *Computer Graphics Forum*. 2021. V. 40. P. 423–434. doi: 10.1111/cgf.14318
6. Jadaun V., Nitin R.S. An application of soliton solutions of a differential equation in the progression of aortic dissection. *Mathematical Methods in the Applied Sciences*. 2023. doi: 10.1002/mma.9565
7. Emerel L., Thunes J., Kickliter T., Billaud M., Phillippi J.A., Vorp D.A., Maiti S., Gleason T.G. Predissection-derived geometric and distensibility indices reveal increased peak longitudinal stress and stiffness in patients sustaining acute type A aortic dissection: Implications for predicting dissection. *The Journal of Thoracic and Cardiovascular Surgery*. 2018. V. 158. № 2. P. 355–363. doi: 10.1016/j.jtcvs.2018.10.116
8. Lipovka A.I., Karpenko A.A., Chupakhin1 A.P., Parshin D.V. Strength properties of abdominal aortic vessels: Experimental results and perspectives. *Journal of Applied Mechanics and Technical Physics*. 2022. V. 63. No. 2. P. 251–258. doi: 10.1134/S0021894422020080
9. Carew T.E., Vaishnav R.N., Patel D.J. Compressibility of the arterial wall. *Circulation Research*. 1968. V. 23. № 1. P. 61–68. doi: 10.1161/01.RES.23.1.61
10. Skacel P., Bursa J. Compressibility of arterial wall – Direct measurement and predictions of compressible constitutive models. *Journal of the Mechanical Behavior of Biomedical Materials*. 2019. V. 90. P. 538–546. doi: 10.1016/j.jmbbm.2018.11.004
11. Peterson L.H., Jensen R.E., Parnell J. Mechanical properties of arteries *in vivo*. *Circulation Research*. 1960. V. 8. № 3. P. 622–639. doi: 10.1161/01.RES.8.3.622
12. Skacel P., Bursa J. Poisson's ratio and compressibility of arterial wall – Improved experimental data reject auxetic behaviour. *Journal of the Mechanical Behavior of Biomedical Materials*. 2022. V. 131. Article No. 105229. doi: 10.1016/j.jmbbm.2022.105229
13. Meyers M.A., Chawla K.K. *Mechanical Behavior of Materials*. Cambridge University Press, 2008. 856 p.
14. Chuong C., Fung Y. Three-dimensional stress distribution in arteries. *Journal of Biomechanical Engineering*. 1983. V. 105. № 3. P. 268–274. doi: 10.1115/1.3138417
15. Bagayev S.N., Zakharov V.N., Markel A.L., Medvedev A.E., Orlov V.A., Samsonov V.I., Fomin V.M. Optimal structure of arterial vessel walls. *Doklady Physics*. 2004. V. 49. No. 9. P. 530–533. doi: 10.1134/1.1810580.
16. Medvedev A.E., Samsonov V.I., Fomin V.M. Rational structure of blood vessels. *Journal of Applied Mechanics and Technical Physics*. 2006. V. 47. No. 3. P. 324–329. doi: 10.1007/s10808-006-0059-3
17. Baek S., Gleason R.L., Rajagopal K.R., Humphrey J.D. Theory of small on large: potential utility in computations of fluid-solid interactions in arteries. *Computer*

Methods in Applied Mechanics and Engineering. 2007. V. 196. № 31–32. P. 3070–3078. doi: 10.1016/j.cma.2006.06.018

18. Ferruzzi J., Vorp D.A., Humphrey J.D. On constitutive descriptors of the biaxial mechanical behaviour of human abdominal aorta and aneurysms. *Journal of the Royal Society Interface*. 2011. V. 8. № 56. P. 435–450. doi: 10.1098/rsif.2010.0299
19. Amabili M., Karazis K., Mongrain R., Païdoussis M.P., Cartier R. A three-layer model for buckling of a human aortic segment under specific flow-pressure conditions. *International Journal for Numerical Methods in Biomedical Engineering*. 2012. V. 28. № 5. P. 495–512. doi: 10.1002/cnm.1484
20. Holzapfel G.A., Gasser T.C., Ogden R.W. A new constitutive framework for arterial wall mechanics and a comparative study of material models. *Journal of Elasticity and the Physical Science of Solids*. 2000. V. 61. № 1. P. 1–48. doi: 10.1023/A:1010835316564
21. Holzapfel G.A., Gasser T.C., Stadler M. A structural model for the viscoelastic behavior of arterial walls: Continuum formulation and finite element analysis. *European Journal of Mechanics, A/Solids*. 2002. V. 21. № 3. P. 441–463. doi: 10.1016/S0997-7538(01)01206-2
22. Holzapfel G.A., Sommer G., Gasser C.T., Regitnig P. Determination of layer-specific mechanical properties of human coronary arteries with nonatherosclerotic intimal thickening and related constitutive modeling. *American Journal of Physiology-Heart and Circulatory Physiology*. 2005. V. 289. № 5. P. H2048–H2058. doi: 10.1152/ajpheart.00934.2004
23. Gasser T.C., Ogden R.W., Holzapfel G.A. Hyperelastic modelling of arterial layers with distributed collagen fibre orientations. *Journal of the Royal Society Interface*. 2006. V. 3. № 6. P. 15–35. doi: 10.1098/rsif.2005.0073
24. Nemavhola F., Pandelani T., Ngwangwa H. Fitting of hyperelastic constitutive models in different sheep heart regions based on biaxial mechanical tests. *Russian journal of biomechanics*. 2022. No. 2. P. 19–30. doi: 10.15593/RZhBiomeh/2022.2.02
25. Giudici A., Khir A.W., Szafron J.M., Spronck B. From uniaxial testing of isolated layers to a tri-layered arterial wall: A novel constitutive modelling framework. *Annals of Biomedical Engineering*. 2021. V. 49. № 9. P. 2454–2467. doi: 10.1007/s10439-021-02775-2
26. Kozlov V.A., Nazarov S.A. Asymptotic models of anisotropic heterogeneous elastic walls of blood vessels. *Journal of Mathematical Sciences*. 2016. V. 213. № 4. P. 561–581. doi: 10.1007/s10958-016-2725-1
27. Chuong C.J., Fung Y.C. Three-dimensional stress distribution in arteries. *Journal of Biomechanical Engineering*. 1983. V. 105. № 3. P. 268–274. doi: 10.1115/1.3138417
28. Choi H.S., Vito R. Two-dimensional stress-strain relationship for canine pericardium. *Journal of Biomechanical Engineering*. 1990. V. 112. № 2. P. 153–159. doi: 10.1115/1.2891166
29. Ngwangwa H., Pandelani T. Msibi M., Mabuda I., Semakane L., Nemavhola F. Biomechanical analysis of sheep oesophagus subjected to biaxial testing including hyperelastic constitutive model fitting. *Heliyon*. 2012. V. 8. № 5. P. 1–10. doi: 10.1016/j.heliyon.2022.e09312
30. Roy D., Kauffmann C., Delorme S., Lerouge S., Cloutier G., Soulez G. A literature review of the numerical analysis of abdominal aortic aneurysms treated with endovascular stent grafts. *Computational and Mathematical Methods in Medicine*. 2012. V. 2012. № 820389. P. 1–16. doi: 10.1155/2012/820389
31. Raghavan M.L., Webster M.W., Vorp D.A. *Ex vivo* biomechanical behavior of abdominal aortic aneurysm: Assessment using a new mathematical model. *Annals of Biomedical Engineering*. 1996. V. 24. № 5. P. 573–582. doi: 10.1007/bf02684226

32. Skripachenko K.K., Golyadkina A.A., Morozov K.M., Chelnokova N.O., Ostrovsky N.V., Kossovich L.Y. Biomechanical patient-oriented analysis of influence of the aneurysm on the hemodynamics of the thoracic aorta. *Russian journal of biomechanics*. 2019. Vol. 23, No. 4. P. 526–536. doi: 10.15593/RZhBiomeh/2019.4.03
33. Shi Y., Zhu M., Chang Y., Qiao H., Liu Y. The risk of stanford type-A aortic dissection with different tear size and location: a numerical study. *BioMedical Engineering OnLine*. 2016. V. 15. № 128. P. 531–544. doi: 10.1186/s12938-016-0258-y
34. Li Z.Y., U-King-Im J., Tang T.Y., Soh E., See T.C., Gillard J.H. Impact of calcification and intraluminal thrombus on the computed wall stresses of abdominal aortic aneurysm. *Journal of Vascular Surgery*. 2008. V. 47. № 5. P. 928–935. doi: 10.1016/j.jvs.2008.01.006
35. Kumara J., Faye A. Prediction of failure envelope of calcified aneurysmatic tissue. *Procedia Structural Integrity*. 2022. V. 42. P. 806–812. doi: 10.1016/j.prostr.2022.12.102
36. Wang L., Roper S.M., Hill N.A., Luo X. Propagation of dissection in a residually-stressed artery model. *Biomechanics and Modeling in Mechanobiology*. 2017. V. 16. P. 139–149. doi: 10.1007/s10237-016-0806-1

Received 26.12.2023.
Published 02.01.2024.